PERIÓDICO TCHÊ QUÍMICA
ARTIGO ORIGINAL

ESTUDO DAS PROPRIEDADES TERMOFÍSICAS E FÍSICO-MECÂNICAS DE FERRO FUNDIDO DE ALTA LIGA DE ALUMÍNIO CHYU22SH

STUDY OF THE THERMOPHYSICAL AND PHYSICAL - MECHANICAL PROPERTIES OF HIGH-ALLOYED ALUMINUM CAST IRON CHYU22SH

ИССЛЕДОВАНИЕ ТЕПЛОФИЗИЧЕСКИХ И ФИЗИКО-МЕХАНИЧЕСКИХ СВОЙСТВ ВЫСОКОЛЕГИРОВАННОГО АЛЮМИНИЕВОГО ЧУГУНА ЧЮ22Ш

ZHUMADILOVA, Zhanar O.[1]; KALDYBAYEVA, Saule T.[2]; NURULDAEVA, Gulzhan Zh.[3]; KUMAR, Dauren B.[4]

[1,3] Kazakh National Research Technical University named after K. I. Satpayev (Satbayev University), Institute of Architecture and Civil Engineering, 22 Satpayev Str., zip code 050013, Almaty – Republic of Kazakhstan (phone: +77771388677)

[2,4] Al-Farabi Kazakh National University, 71 Al-Farabi Avenue, zip code 050040, Almaty Republic of Kazakhstan

** Corresponding author*
e-mail: zhanar_85@mail.ru

Received 26 June 2019; received in revised form 05 November 2019; accepted 16 November 2019

RESUMO

Ligas de alta liga, nas quais cromo e níquel são elementos de liga, são amplamente utilizados como materiais resistentes ao calor. Seu conteúdo total em ligas resistentes ao calor atinge 30% ou mais. No entanto, a vida útil das peças de trabalho feitas de ligas resistentes ao calor é limitada. Além disso, quanto maior a temperatura de operação, menor é a vida útil. Isso leva ao aumento de custos para manter as unidades em condições de trabalho. Exemplos dessas peças são a grade de máquinas de aglomeração, detalhes de plantas de caldeiras, fornos de torrefação, aquecimento e fusão de vidro, moldes de fundição, coletores de exaustão de motores forçados de automóveis, entre outros exemplos. A esse respeito, reduzir o custo de produtos resistentes ao calor, mantendo suas características operacionais e vida útil, torna-se uma necessidade. Uma das opções promissoras para resolvê-lo é fabricar essas peças de ferro fundido de alumínio resistente a altas temperaturas CHYU22SH (CHYU22SH - ferro fundido padrão). As peças fundidas de ferro fundido CHYU22SH diferem, em primeiro lugar, pela resistência ao calor a altas temperaturas no ar (até 1100 ° C) e em meios contendo enxofre, dióxido de enxofre, óxidos de vanádio e vapor de água. Além disso, elas podem operar funcionalmente como um produto resistente ao desgaste, com alta resistência a temperaturas normais e elevadas. O trabalho apresenta as propriedades térmicas e mecânicas da fundição, bem como os resultados da análise microestrutural de ferros fundidos de alta liga de alumínio. Os resultados de análises e testes mostram que a liga de ferro fundido CHYU22SH pode ser obtida por fundição com paredes longas com uma espessura de 4 mm, sem defeitos externos e internos. Ao fazê-lo, as peças fundidas têm uma estrutura uniforme, propriedades mecânicas altas e estáveis, além de serem inferiores em ~ 17-24% em peso do que um ferro fundido semelhante. Os resultados de estudos laboratoriais experimentais - industriais de laboratório confirmam a influência das condições de solidificação nos parâmetros da estrutura do ferro fundido CHYU22SH.

Palavras-chave: *análise microestrutural, teste tecnológico, teste em escala piloto, peça fundida, capacidade de aquecimento.*

ABSTRACT

Highly alloyed alloys, in which expensive chromium and nickel are alloying elements, are widely used as heat-resistant materials. Their total content in heat-resistant alloys reaches 30% or more. However, the life of working parts made of heat-resistant alloys is limited. Moreover, the higher the operating temperature, the shorter it is. This leads to increased costs for maintaining the units in working condition. Examples of such parts are the grate of agglomeration machines, details of boiler plants, roasting, heating, and glass melting furnaces,

DOI: 10.52571/PTQ.v16.n33.2019.45_Periodico33_pgs_30_40.pdf

casting molds, exhaust manifolds of forced automobile engines, etc. In this regard, reducing the cost of heat-resistant products, while maintaining their operating characteristics and life, becomes very actuality. One of the promising options to solve it is to manufacture these parts made of high-alloyed heat-resistant aluminum cast iron CHYU22SH (CHYU22SH - standard cast iron). Castings made of cast iron CHYU22SH differ, first of all, by being heat resistance at high temperatures in air (up to 1100 °C) and in media containing sulfur, sulfur dioxide, oxides of vanadium, and water vapor. In addition, they can functionally operate as a wear-resistant product having high strength at normal and elevated temperatures. The paper presents the thermal and mechanical properties of casting, as well as the results of microstructure analysis of aluminum cast irons. The results of analyses and tests show that cast iron CHYU22SH can be obtained by casting with long walls of a thickness of 4 mm without external and internal defects. By doing so the castings have a uniform structure, high and stable mechanical properties, as well as lower by ~17-24% weight than similar cast of gray iron. The results of experimental - industrial testing laboratory studies confirm the influence of solidification conditions on the parameters of the structure of cast iron CHYU22SH.

Keywords: *microstructural analysis, technological test, pilot-scale testing, cast part, heat capacity.*

АБСТРАКТ

В качестве жаростойких материалов широко применяют в основном высоколегированные сплавы, в которых легирующими элементами являются дорогостоящие хром и никель. Общее содержание их в жаростойких сплавах достигает 30 % и более. Тем не менее, срок жизни рабочих деталей из жаростойких сплавов ограничен. Причем, чем выше рабочие температуры, тем он короче. Это обусловливает повышенные затраты на поддержание агрегатов в рабочем состоянии. Примерами таких деталей являются колосники агломерационных машин, детали котельных установок, обжиговых, нагревательных и стекловаренных печей, формы для литья, выхлопные коллекторы форсированных автомобильных двигателей и др. В связи с этим, снижение затрат на жаростойкие изделия при сохранении их рабочих характеристик, в том числе и срока службы, становится весьма актуальной задачей. Одним из перспективных вариантов ее решения является изготовление таких деталей из высоколегированного алюминиевого жаростойкого чугуна ЧЮ22Ш (ЧЮ22Ш-стандартный чугун). Отливки из чугуна ЧЮ22Ш отличаются, прежде всего, жаростойкостью при высоких температурах как в воздушной среде (до 1100° С) так и в средах, содержащих серу, сернистый газ, окислы ванадия и пары воды. Кроме того, они функционально могут работать и как износостойкие изделия, имеющие высокую прочность при нормальной и повышенной температурах. В работе представлены теплофизические, литейные и механические свойства, а также результаты микроструктурного анализа алюминиевых чугунов. Результаты анализов и лабораторных испытаний свидетельствуют о том, что из чугуна ЧЮ22Ш могут быть получены отливки с протяженными стенками толщиной 4 мм без наружных и внутренних дефектов. При этом они имеют однородную структуру, высокие и стабильные показатели механических свойств, а также меньшую на ~ 17 - 24 % массу, чем аналогичная отливка из серого чугуна. Результаты опытно – промышленного опробования подтверждают данные лабораторных исследований о влиянии условий затвердевания отливок на параметры структуры чугуна ЧЮ22Ш.

Ключевые слова: *микроструктурный анализ, технологическая проба, опытно–промышленные опробования, литая деталь, теплоемкость.*

INTRODUCTION

Design technology in modern foundries uses a variety of commonly used software packages for modeling of mold filling, solidification, and cooling of castings. Using these programs help to solve many technological problems. One of the stages of modeling in such programs (LVMFlow, ProCAST, Polygon) is the choice of the alloy from the database. Unfortunately, iron CHYU22SH is not present in any of the databases of the above-mentioned programs. Accordingly, casting simulation in the production of castings from this alloy is not possible. In the database for jobs of preparing a new alloy, it is necessary to know some of its properties, including its thermophysical properties.

Heat-resistant materials are widely used in most high alloys, which are expensive alloying elements chromium and nickel. The total content of heat-resistant alloys then reaches 30% or more. However, the life of the working parts of the heat-resistant alloys is limited. Moreover, the higher its operating temperatures, the shorter its life. This results in a higher cost to maintain the units in working condition. Examples of such devices are grate sintering machines, parts of boilers, kilns, glass furnaces and heaters, molds,

exhaust manifold-boosted automobile engines.

MATERIALS AND METHODS

2.1 Thermophysical properties

Thermophysical properties of cast iron are needed for computer simulation of melt filling of the cavity mold, solidification, and cooling of the castings in order to select the best technology option of obtaining them without having casting defects. However, such information on cast iron CHYU22SH is virtually non-existent. In (Kovalevich, 1991, Zhuravlev, 1981) writing indicates that the specific heat of aluminum cast-iron type CHYU22SH at normal temperature is lower than that of gray and ductile cast irons, with increasing temperature as the thermal conductivity of aluminum iron increases at a time when the undoped iron is reduced (Ten, 2015). Therefore, at high temperatures (900 – 1000 °C) a superior thermal conductivity CHYU22SH GCI (gray cast iron) and HCING (high-strength cast iron with nodular graphite) are produced (Kumanin, 1976).

It was measured the specific heat, thermal conductivity, and thermal diffusivity of CHYU22SH iron in the temperature range 500 - 1000 °C. Experiments were conducted in the laboratory of Satbayev University on the devices NETZSCH DSC 404 C Pegasus (to determine the heat capacity) and the NETZSCH LFA 457 Micro-Flash® (for the determination of heat and thermal diffusivity). Tests were conducted on specimens made of strong cast samples and had a density of 5909 kg/m^3. Sample sizes had a diameter of 12.700 mm and a thickness of 3.1580 mm (Tanski, 2016; Jiang, 2016, Lagunov, 1980). The results are shown in Table 1 as the mean values of five measurements.

According to our data the specific heat of cast iron CHYU22SH increases with increasing temperature to 536 J/kg K at 500 °C and 585 J/kg K at 1000 °C, which is comparable with that of the undoped cast iron with spheroidal graphite (nodural cast iron with nodular graphite, 570 - 592 in 500 °C and 595-649 at 1000 °C).

Thermal conductivity of cast iron CHYU22SH increases with increasing temperature and is more significant than the heat - from 12.64 W/m·K at 500 °C to 15.53 W/m·K at 1000 °C. The obtained values are much smaller than given in (Kaldybayeva, 2011): 16.28 W/m K at 200 °C and 26.75 W/m·K at 500 °C. At the (Kaldybayeva, 2011) same temperature (500 °C) values, differ by more than double. It is assumed that in the figures more reliable heat, as obtained on modern equipment, is shown with each value measured five times and performed in a wide range of temperatures. On this basis, (Kaldybayeva, 2011) can assume that the aluminum cast iron CHYU22SH has a thermal conductivity approximately 3 times lower than the undoped iron CING (cast iron with nodular graphite) with ferritic metal matrix, which at 400 °C has a thermal conductivity of 38 W/(m·K). Since the thermal conductivity in undoped iron decreases with increasing temperature, while the cast iron CHYU22SH is on the rise at the operating temperature of 1000 - 1100 °C, this difference should be much reduced (Utepov, 2014; Ten, 2016; Safronov, 2017, Kerzhentsev, 1971).

Thermal diffusivity in iron CHYU22SH increases monotonically with $4 \cdot 10^{-6}$ m^2/s to $4.5 \cdot 10^{-6}$ m^2/s with increasing temperature from 500 to 1000 °C. The (Kaldybayeva, 2011) lack of published data does not allow comparing the obtained values. In undoped cast iron CING (cast iron with nodular graphite) the indicator is $(5.5\text{-}6.5) \cdot 10^{-6}$ m^2/s at 600 °C and $(5.0\text{-}5.6) \cdot 10^{-6}$ m^2/s at 800 °C. Comparison of the data shows that the iron CHYU22SH at 600 and 800 °C has a thermal conductivity at 33 and 20% lower, respectively, but at higher temperatures and thermal irons CHYU22SH and CING can be slightly different (Kaldybayeva, 2011; Stefanescu, 2017; Utepov, 2017; Prasad, 2018; Martin, 2016, Sitko, 2017).

To assess the possibility of obtaining a particular set of alloy castings its casting properties such as fluidity, shrinkage, the mechanical effect of the distance, and the distance of the profits are needed to be known.

2.2. Casting properties

To assess the possibility of obtaining a particular set of alloy castings, we need to know its casting properties such as fluidity, shrinkage, the mechanical effect of the distance, and the distance of the profits.

The results of determining the parameters of fluidity and shrinkage of cast iron CHYU22SH are shown in Table 2.

As can be seen, the spiral fluidity test values that are measured are comparable with published data; however, free casting shrinkage is less than 1.5 times when compared with the data (Tanski, 2016). In (Utepov, 2014; Zhang, 2018; Paul, 2018) with increasing carbon content in the

aluminum cast iron above 2%, a decrease of fluidity occurs as a result of the graphite in the melt.

Preshrinkage expansion of high-alloyed aluminum cast iron CHYU22SH is much smaller compared with that of the undoped cast iron (0.07%) (Galdin, 1992).

2.2.1. Power options castings

There is a need for supply of castings devoid of the formation of these defects in the form of shrinkage cavities and shrinkage porosity. The latter is a consequence of the formation in the inner sections of the casting of closed areas in which the solidification of the alloy occurs under conditions of full or partial nutritional deficiency (Kurdyumov, 1996; Galdin, 1992).

Casting alloys are characterized by varying propensity for the formation of shrinkage defects. The share of volume shrinkage, which is found in the form of shrinkage cavity and porosity shrinkage, mainly depends on the interval of crystallization of the alloy and the casting cooling intensity. Alloys that have a small range of crystallization shrinkage of its volume mainly found in the form of shrinkage cavities are required. Alloys with a wide range of crystallization of a large or a significant portion of the volumetric shrinkage found in the form of shrinkage porosity are also required. At the same time with increasing intensity of the cooling sections of the casting a high temperature gradient is formed, due to the width of the two-phase solid-liquid region at the final stage of solidification, which is narrow and, consequently, reduces the proportion of volume shrinkage that is found in the form of shrinkage porosity (Galdin, 1992; Vasiliev, 1976; Kavalevich, 1991). All other things being the same, the tendency of the alloy for forming shrinkage defects in the form of shrinkage cavities and shrinkage porosity increases with an increase in its volumetric shrinkage (Table 3).

In most cases, high volumetric shrinkage results in the formation of shrinkage in the castings because of unacceptable defects in the form of internal shrinkage cavities and shrinkage porosity. It is necessary to provide good quality castings to eliminate them. This is achieved by setting profits in the right place, required quantity, and sufficient size. At the same time directional solidification condition in which the solidification front moves sequentially from the end parts (peripheral areas) to the inside, from thin to thick walls, and the latter to the profits must necessarily be provided. The number and size of the profits should be necessarily minimum. This minimizes the consumption of metal in the profit and complexity of their subsequent separation from the castings.

To solve such a complex task requires knowledge of the power setting of castings, that is, the distance (radius) L_{dp} of the food arrived, the distance of the mechanical effect of $L_{me,}$ and the total area of effective supply $L_{\Sigma} = L_{dp} + L_{me}$. These parameters are estimated as multiples of the casting thickness t or the reduced-thickness R = V/S, where V and S, are, respectively, the amount fed host (casting) and surface cooling. These strongly depend on the type of alloy (Table 4).

Regarding the influence of the thickness of the casting on these parameters, we have only a few observations. For high-alloy cast iron, aluminum CHYU22SH data on the parameters of supply castings are completely absent. However, this iron has a high volumetric shrinkage (3.2-7.0% according to (Kovalevich, 1991) 4.5-8%, according to (Stefanescu, 2017; Jiang, 2016; Shayakhmetov, 2014)) and because of the casting during solidification, it will become malnourished. But without knowing the parameters of supply castings from this alloy, we cannot properly organize the directional solidification.

Therefore, we require a detailed study of the power settings of cast iron CHYU22SH casting. To do this, we developed a 2-, 3-, and 4-lobed squared test. Figure 1 gives an example of a 2-blade test. The sample consists of a riser - a profit 1, profit platform (base) 2, and immediately squared tests 3.

Profit for the samples was calculated by the method of Namur – Shklennik (Equation 1):

$$V_p = m \cdot \xi \cdot R_{TU}{}^3 \cdot (1+\beta)^3 \cdot y \cdot z + 3 \cdot \beta \cdot V_f \quad \text{(Eq.1)}$$

where: m - is the coefficient of non-identity of the metal in the casting temperature and profit by the end of fill or a dimensionless coefficient depending on the distance between the profit and the place of supply of metal to the casting:

ξ - dimensionless coefficient configuration profits (Equation 2):

$$\xi = \frac{S_{ef}{}^3}{V_p{}^2} \quad \text{(Eq.2)}$$

where S_{ef} - is the surface area of the profits, in contact with the form;

V_p - is the amount of profit;

R_{TU} - is the effective reduced thickness of the thermal unit (Equation 3):

$$R_{TU} = \frac{V_{TU}}{S_{TU.ef}} \qquad \text{(Eq.3)}$$

V_{TU} - is the amount of thermal unit;

$S_{TU.ef}$ - is the effective surface area of the thermal unit;

β - is the volumetric shrinkage of cast iron;

y - is the coefficient of a non-identity configuration of the casting and profits - a dimensionless coefficient that takes into account the relative length of time of solidification thermal unit and profits, depending on their configuration (Equation 4):

$$y = \frac{m_{sol.TU}}{\tau_{sol.profit}} \qquad \text{(Eq.4)}$$

z - is the coefficient of the cooling cooling conditions are not identical to the profit and and metal casting (Equation 5):

$$z = \frac{b_{f.p.}}{b_{f.TU}} \qquad \text{(Eq.5)}$$

where $b_{f.p}$ and $b_{f.TU}$ are thermal storage capacity of the form in contact with a profit and thermal unit;

V_f - is the amount of form or the part for which the calculated profit.

The thickness of the bars t was 6, 12, 24, 30, 36, 42, and 48 mm with a width of 100 mm. The length of the bars ℓ is selected from the principle of sufficiency. At the same time, we believe that the high-alloyed aluminum ductile iron CHYU22SH power distance is approximately the same as that of ductile iron ($L\Sigma \approx 6 \cdot t$). Based on this, it is taken (with a small margin) $\ell = 7 \cdot t$. These samples were cast in sand - clay raw form.

Of the cast samples obtained template, we customize the individual. To do this, blocks were cut in half along the longitudinal plane. Milling was done to the plane of the section for the identified areas of porosity on the plate (Figure-2).

To do this, we have tried various methods, including visual, ultrasonic, and hardness measurement methods. The ultrasonic method for determination of shrinkage defects did not give stable results, probably due to the presence of graphite inclusions and the presence of oxide prisoner. The visual method can detect only the surface porosity that is manifested, which is not always, and the hidden porosity remains unaccounted for. The adequate results were obtained using the method of measuring the Rockwell hardness (HRC). The hardness was measured on the centre line of the plate at distances that were multiples of the petal thickness t (Figure-3).

The distance of the mechanical effect L_{TU} and the distance from the feed arrived L_{dp}, and their sum is the total distance of the effective power $L_{\Sigma} = L_{dp} + L_{me}$ measured by the length of the dense metal part and the end, respectively.

Cast iron CHYU22SH (Table 5) was smelted in an induction crucible furnace HFICF - frequency - 0.06 with the main lining (HFICF - high-frequency induction crucible furnace).

Following the modification of cast iron was poured into molds heated to 800 °C, with a melt temperature ranging 1420 - 1450 °C.

After solidification, it was cooled in a form completely. Then to relieve stress, reduce hardness, and improve the workability, it was subjected to annealing, and after heat treatment produced crop gating system and finishing operations (Tanski, 2016, Saburov, 1967).

The molded piece "exhaust manifold" thus made is presented in Figure 4.

Visual inspection revealed no visible external defects in the casting foundry. A plate control, cut from the castings showed their lack of these and internal defects.

We evaluate the mechanical properties of cast iron with cast collector bars (Figure-5).

Before machining the bars were subjected to heat treatment. Then cylindrical samples were produced for mechanical testing having a diameter of 8 mm and a gauge length of 50 mm.

Tensile tests were performed on the instrument Zwick/Roell Z250. The hardness of iron was measured on the instrument Wolpert Hardness Taster 930, at a load of 187 kg. The results are shown in Table 6.

The results of the mechanical tests show that the resulting iron CHYU22SH has a tensile strength of ~390 MPa, which is 30% above the lower margin in accordance with GOST 7769-02 (Government standard). The hardness of iron (~ 270 HB) is within the regulated values, but closer to the lower limit. In this case, the yield stress of iron is ~340 MPa, elongation 0.6%, and modulus of normal elasticity ~160 GPa. The results obtained show that the tensile strength of

aluminum-smelted iron corresponds to the ultimate strength VCH35 – VCH40 (standard cast iron), yield strength, respectively, CVH50 exists and corresponds to the hardness of VCH100 (standard cast iron) (G. Nuruldaeva, 2019; Zhang, 2018).

For the structure of cast iron were performed on a microscope Neophot 21 firms ZEISS JENA at different magnifications. It consists of a metal matrix and uniformly distributed in its compact form of graphite inclusions (Figure-6a).

The metal matrix is doped with aluminum ferrite - *α* phase, which is uniformly distributed in the iron - aluminum carbide ε phase (Figure-6, *b,* and *c*).

Graphite inclusions (in accordance with GOST 3443-01) mainly take the form of NGf5 and only partially NGf4 (NGf - nodular graphite form). The size of graphite inclusions should be in the range of 30-60 microns.

3. RESULTS AND DISCUSSION

The results of analyses and tests show that cast iron CHYU22SH can be obtained by casting with long walls of a thickness of 4 mm without external and internal defects. By doing so, the castings have a uniform structure, high and stable mechanical properties, as well as lower by 17-24% weight than similar cast of gray iron.

4. CONCLUSIONS

1. Thus, a combination of innovative and traditional casting technology allows for a short time to develop manufacturing technology options and assess the quality indicators of the castings of various alloys, including decreased fluidity, high linear and volumetric shrinkage, as well as susceptibility to saturation of the gases and dust production. This integrated approach allows us not only to speed up technological preparation for the production of castings but also reduce costs for manufacturing and finishing of expensive mold tools. An example of such an approach is to develop practical applications for future technology for high-quality cast iron CHYU22SH cast parts "exhaust manifold" with increased operational and consumer properties.

2. Thus, the results of experimental - industrial testing laboratory studies confirm the influence of solidification conditions on the parameters of the structure of cast iron CHYU22SH. Application of the developed technology allows obtaining high-quality recommendations casting a thin (4 mm) and thick, without shrinkage defects in origin, are guaranteed to have the required degree of spheroidization of graphite inclusions, high and stable mechanical properties, as well as a smaller mass.

5. ACKNOWLEDGMENTS:

The authors are grateful to the leadership of the Kazakh National Research Technical University named after K. I. Satpayev (Satbayev University) for creating the conditions for carrying out this work.

6. REFERENCES:

1. Ten, E. B., Bazlova, T. A., Likholobov, E. Y. Effect of Out-of-Furnace Treatment on the Structure and Mechanical Properties of Steel 110G13l // Metal Science and Heat Treatment. – Volume 57. Issue 3-4. 146-150 p.p. 1 July 2015.
2. Kumanin I. B. Reviews of casting processes. 216 p. Mechanical Engineering, Moscow. 1976.
3. Kaldybayeva S. Research of Crystallization of Aluminum cast iron. Journals of Minerals & Materials Characterization & Engineering., Vol.10, No.13 -2011. pp. 1197-1203.
4. Kurdyumov A. V. Pikunov M. V., Chursin V. M., Bibikov E. L. Casting of non-ferrous alloys. 504 p. Moscow Inst.Steel&Alloys, Moscow, 1996.
5. Galdin N. M., Chistyakov V. V., Shatulsky A. A. Gating system and profit for shaped castings. 256 p. Mechanical Engineering, Moscow, 1992.
6. Vasiliev E. A. Castings of ductile cast iron. 239 p. Mechanical Engineering, Russia, 1976.
7. Kavalevich E. V. Aluminum cast iron. Handbook. Editor A. D. Sherman and A. A. Zhukov. 576 p. Moscow: Metallurgy, Russia, 1991.
8. Stefanescu D. M., Alonso G., Larranaga P. Reexamination of crystal growth theory of graphite in iron-carbon alloys// Acta Materialia, vol. 139 - 2017.- pp.109-121.
9. Utepov E. B., Ten E. B., Zhumadilova Z.O., Smailova G. A., Shevtsova V.S. Damping Metallic materials with a nanostructured Coating // Metallurgist. – Volume 60. – Issue 9-10, 1. – January 2017. – pp. 961-966.
10. Tanski T, Labisz K, Krupinska B. Analysis of crystallization kinetics of cast aluminum-silicon alloy// Journal of thermal analysis and

calorimetry, vol. 123 - 2016. - pp. 63-74.
11. Utepov E. B., Madizhanova A. T., Malgazhdarova M. K., Egemova Sh. B. Research of acoustic properties of alloyed steels. Metallurgist. 2014. Volume 8. pp. 92-95.
12. Ten, E. B., Kol, O. A. Action of protective coatings on surface carbonizing of steel castings // Chernye Metally. – Issue 5. – 1 May 2016. – pp. 35-39.
13. Safronov N. N., Kharisov L. R., Safronov G. N. Aluminum cast iron with compacted inclusions of graphite from dispersed production waste// published in Tekhnologiya Metallov, 2017, No. 4, pp. 2–5.
14. Shayakhmetov B. K., Kimanov B. M., Ten E. B., Isagulov A. Z., Zholdubaeva Z. D., Isagulova D. A. Gravimetric and Dilatometric research of elements action on three dimensional filter by thermal effects // Metalurgija. – vol. 53. – No, 1. – 2014. – pp. 44-46.
15. Zhang J, Xia S, Ye S. Experimental investigation on the noise reduction of an axial piston pump using free-layer damping material treatment// published in Applied Acoustics– vol. 139 – 2018- pp. 1-7.
16. Paul P, Raja P, Aruldhas P. Effectiveness of particle and mass impact damping on tool vibration during hard turning process// Proceedings of the institution of mechanical engineers part b-journal of engineering manufacture, vol. 232 –2018- pp. 776-786.
17. Prasad D, Radha P, Shoba Ch. Optimizing of Wire EDM Parameters for Damping Capacity of Aluminum Alloy // Materials today proceedings, vol. 5 - 2018- pp. 168-169.
18. Zhuravlev V. N., Nikolaev O. I. Mechanical steels. Directory. - M.: Mechanical Engineering, 1981. - 391 p.
19. Kerzhentsev V. V., Dedenko L. G. Mathematical processing and registration of the results of the experiment. - M.: MSU, 1971. - 10 p.
20. Saburov V. P. Effect of the modification on the properties of cast iron casting, aluminum-doped. Casting properties of metals and alloys. Proceedings of the Eleventh 11th Conference on the Theory of casting processes. Edited by B.B. Gulyaev. 267p. Moscow: Publishing House "Science" (1967).
21. G. Nuruldaeva, Zh. Zhumadilova, S. Kaldybayeva, D. Kumar. Dissipative properties of the high alloy aluminum cast iron CHYU22SH. The scientific and technical journal "INDUSTRY OF KAZAKHSTAN". No.2 (106) 2019. International code ISSN 1608-8425. P.59. Almaty, RSE "National Center for the Integrated Processing of Mineral Resources of the Republic of Kazakhstan".
22. Martin P, Micheal R. Piezoelectric shunt damping of a circular saw blade with autonomous power supply for noise and vibration reduction// Journal of sound and vibration, vol. 361 -2016- pp. 20- 31.
23. Jiang J, Yue M, Fu H. Phase diagram calculation and experimental research on Fe-12Cr-B-Al alloys// Materrial wissenschaft und werkstoftechnik, vol. 47 - 2016.- pp. 808-814.
24. Lagunov L. F., Osipov G. L. Anti-noise measures in mechanical engineering. - M.: Mechanical Engineering, 1980. - 150 p.
25. Sitko Ye. A., Sukurov B. M., Ospanov Ye., Medvedev O. S. The effect of thermal treatment of converter slags from Balkhash Copper-Smelting plant on their structure and phase composition./ News of the academy of science of the Republic of Kazakhstan. Series of Geology and Technical series. 3 (423), 2017, № 3, p. 175-184.

Table 1. *Thermophysical properties of cast iron CHYU22SH*

Name of property	**Temperature, °C**					
	500	600	700	800	900	1000
Specific heat capacity $C_{c.i}$, J /(kg·K)	536 ± 0.001	549 ± 0.001	559 ± 0.001	565 ± 0.001	573 ± 0.001	585 ± 0.001
Thermal conductivity $\lambda_{c.i}$, W/(m·K)	12.64 ± 0.028	13.11 ± 0.068	13.64 ± 0.048	14.19 ± 0.136	14,93 ± 0.157	15.53 ± 0.141
Thermal diffusivity $a_{c.i}$, 10^{-6} m^2/s	3.99 ± 0.009	4.04 ± 0.021	4.13 ± 0.014	4.25 ± 0.041	4.41 ± 0.047	4.49 ± 0.041

Table 2. *Fluidity and casting shrinkage of cast iron CHYU22SH (*Ten*, 2016; Safronov, 2017; Shayakhmetov, 2014)*

Fluidity, mm	**Casting shrinkage, %**		**Preshrinkage expension, %**
	Free	**Difficult**	
(525 - 775)/(590-830)	(1.42 – 1.52)/(2.2-2.5) /(2.5-2.8)	(1.26 – 1.47)	0.01/ (0.15-0.35)

Table 3. *Volume shrinkage of casting alloys (%) (Kurdyumov, 1996; Galdin, 1992; Vasiliev, 1976)*

Casting alloys						
Steels	**Cast irons (standard cast irons)**			**Non-ferrous metals**		
	Malleable cast iron	Gray cast iron	HCING (high-strength cast iron with nodular graphite)	Copper	Aluminium	Magnesium
4.1 - 7.0	4.0 - 6.0	1.5 - 3.0	2.0 - 6.0	4.0 - 7.5	3.0 - 6.0	3.4 – 5.0

Table 4. *Power supply castings for different groups of alloys*

Alloys	Area of dense metal expressed in thickness		
	Profit zone	**Mechanical zone**	**Sum**
Carbon steel	(2.0)·t	(2.5)·t	(4.5)t
Copper alloys	(2.0-4.5)t	(3.6-5.8)t	(5.6-10.3)t
Aluminium alloys	(2.5-4.0)t	(4.0-4.5)·t	(6.5-8.5)t
Gray cast iron	-	-	Very large
Cast iron with nodular	-	-	6.0-6.5t
Cast iron CHYU22SH	+	+	+

Table 5. *The chemical compound of the experimental melting of cast iron CHYU22SH (Stefanescu, 2017)*

Element	C	Si	Mn	Al	S	P
Mass, %	1.6 - 2.0	1.3 - 1.5	0.45 - 0.50	21.5 - 3.7	0.01 - 0.02	0.10 - 0.12

Table 6. *Results of mechanical testing of tensile specimens at room temperature*

Number of tests	Ultimate strength σ_B,	Yield strength $\sigma_{o,2}$, MPa	Elongation ε, %	Elastic modulus	Hardness, HB
The requirements of GOST 7769-02	290 least	-	-	-	241 - 364
1	381	334	0.5	148	268.5 *
2	402	347	0.6	176	264.5 *
3	394	342	0.5	161	274.0 *
4	378	328	0.7	151	276.5 *
Averages	389 ± 11	338 ± 8	0.6 ± 0.1	159 ± 13	270.9 ± 14.5

* Mean values of four measurements.
GOST – Government standard.

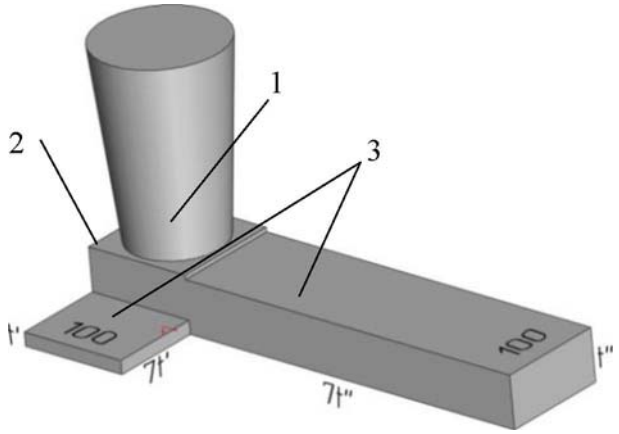

Figure 1. *2^x blade test: 1 - strut-profit, 2 - base, 3 - part of the investigated samples*

Figure 2. *Flow test and preparation for the testing template*

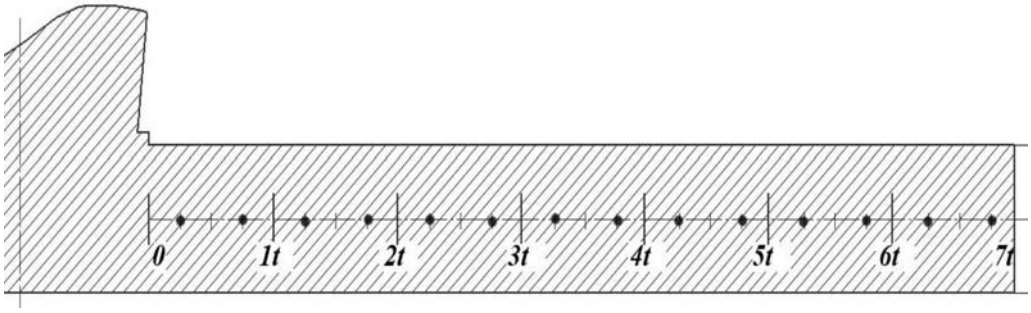

Figure 3. *The scheme of measurement of hardness to determine the parameters of the casting supplies, • - the point of measurement of hardness*

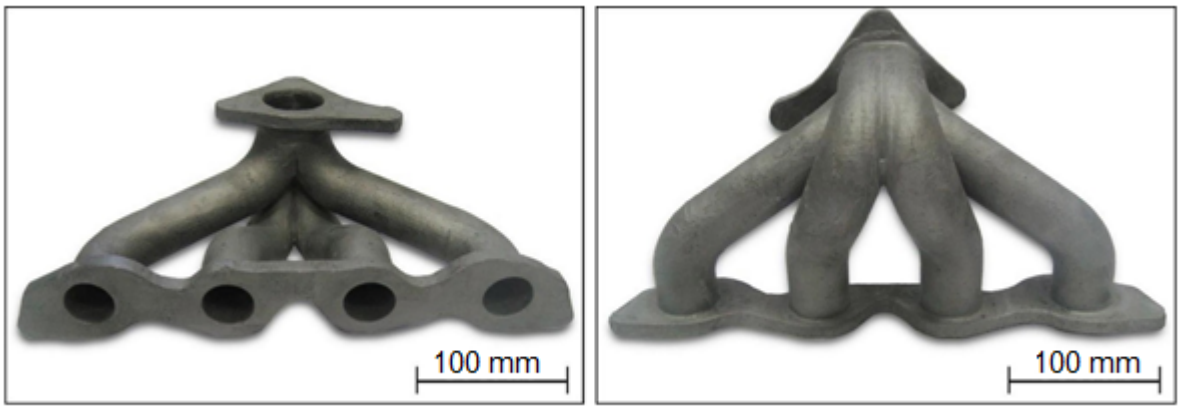

Figure 4. *Cast item "exhaust manifold" of cast iron CHYU22SH*

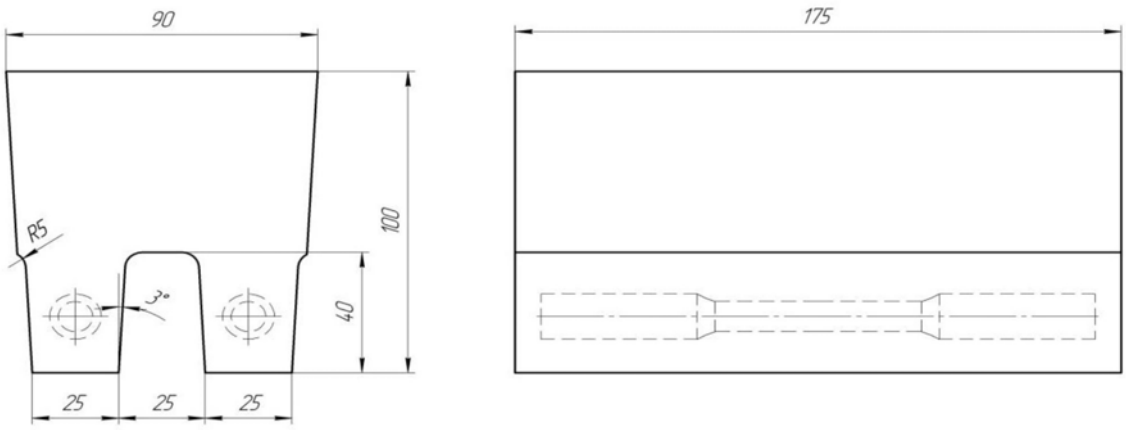

Figure 5. *Cast iron bars to test the mechanical properties*

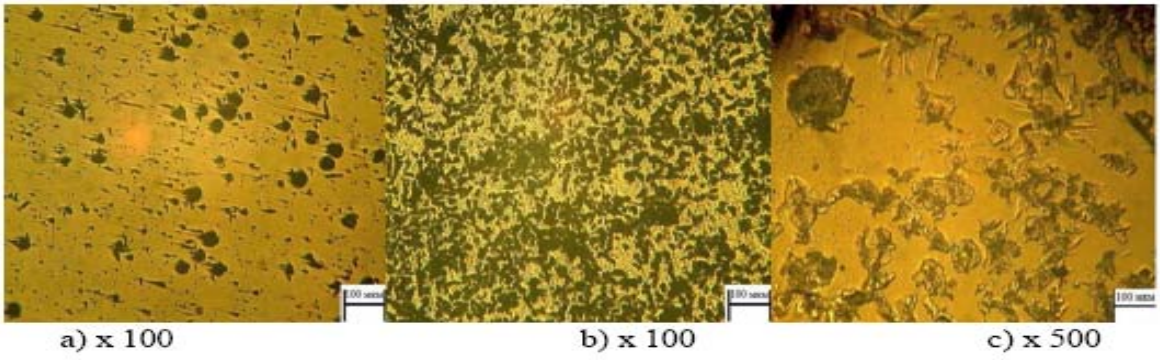

Figure 6. *Structure of the iron CHYU22SH in the samples breaking (a) is not etched; (b) and (c) after etching*